

Formation and development of ventilated supercavity past the disk–cavitator in accelerated motion

V. Moroz¹ • V. Kochin¹ • V. Semenenko¹ • O. Naumova¹

Received: 25 August 2023 / Revised: 18 September 2023 / Accepted: 29 September 2023

Abstract. The work is devoted to both the experimental studies and the computer simulation of the process of formation and development of a ventilated supercavity past the disk-cavitator in accelerated motion from the state of rest to the steady velocity. A series of experiments were carried out in the high-speed experimental tank at the Institute of Hydromechanics of the National Academy of Sciences of Ukraine for various values of the air-supply rate into the cavity. It has been established that the portion type of air-loss from the cavity is always preserved in the case of horizontal accelerated motion, while the air-loss by vortex tubes is always realized in the case of steady motion with the same velocity. In this case, shape of the cross sections of the unsteady cavity is close to circular one along the whole cavity length and at all stages of acceleration. To describe this process, a modified mathematical model is proposed that is based on the G.V. Logvinovich principle of independence of the cavity section expansion. An analysis of the influence of both the immersion depth and the air-supply rate on the process of development of a ventilated supercavity during acceleration has been performed by the way of computer simulation.

Keywords: disk cavitator, ventilated supercavity, accelerated motion, experimental studies, computer simulation.

1. Introduction

The purpose of this work is both the experimental study and the computer simulation of the process of formation and development of a ventilated supercavity in accelerated motion from the state of rest with the specified model acceleration $a = dV/dt > 0$ and the specified volumetric rate of air-supply into the cavity \dot{Q}_{in} . The main factors determining the cavity growth speed are the increasing the flow velocity $V(t)$ and the balance between air-supply into the cavity \dot{Q}_{in} and air-loss from the cavity $\dot{Q}_{out}(t)$.

The laws of air-loss from horizontal ventilated cavities in a steady flow have been studied quite well [1–4]. When calculating unsteady supercavitation flows with low accelerations, these laws are also successfully applied in

the quasi-steady approximation. However, as shown below, their application in the case of accelerated motion with relatively low velocities has its own peculiarities.

The process of formation and development of a cavity during acceleration starting from a state of rest, can be divided into two characteristic time stages. The first stage is from the velocity $V = 0$ to the formation of an initial cavity with the length L_{c0} with relatively low velocity V_0 corresponding to the cavitation number $\sigma = 2(p_w - p_c)/\rho V^2 \approx 0.5$. At the second stage, the model velocity is increased from V_0 up to the specified value V_1 , and the cavity length is increased from L_{c0} up to the specified value L_{c1} .

The processes of the gas-filled cavity formation at the first stage are very complex [5, 6] and cannot be modeled within the framework of the approximation mathematical model based on the G.V. Logvinovich principle of independent of the cavity section expansion [7, 8]. As the experience of applying this mathematical model shows, it gives good results at sufficiently small values of the cavitation number $\sigma < 0.1$ and relatively high values of velocity $V > 10$ m/s when the supercavity has a large aspect ratio.

✉ V. Semenenko
vnsvns60@gmail.com

¹ Institute of Hydromechanics of the National Academy of Sciences of Ukraine, Kyiv, Ukraine

In our works [9, 10], using the method [8], we analyzed the process of accelerating self-propelled models from the starting velocity $V_0 = 10$ m/s to reaching the specified supercavitation flow regime with velocity $V_1 = 120$ m/s. In work [9], the acceleration process was studied under the assumption that the model path on the acceleration distance is rectilinear and horizontal, and the cavity is axisymmetric. It was shown that supercavitating models have a “drag hump” during acceleration, which may be overcome with the help of both the increased starting thrust and the intensive air-supply into the growing cavity in order to accelerate its development. An estimation of the air-supply value on the acceleration distance is given. In work [10], the acceleration process was studied with full consideration of the self-propelled supercavitating model dynamics. Recently, the same mathematical model was used in work [11] to simulate the accelerated and decelerated motion of a supercavitating model, taking into account its maneuvering with the help of hydrodynamic fins. In this case, it was allowed to change the model velocity in a relatively narrow range 50÷60 m/s.

One of the purposes of this work is to check the possibility of applying the approximation mathematical model [8] to simulate the behavior of a growing ventilated cavity at the second stage of its formation. Comparison with the obtained experimental data allows the necessary changes to be made in this mathematical model.

2. Process of formation of a ventilated cavity

Qualitatively, the processes at the initial stage of a cavity formation past a disk during its accelerated motion are described in books [5, 6]. The cavity formation begins with the formation of vapor and gas bubbles in the rarefaction zone past the disk, and in the cores of vortex structures in the wake past the disk. The process of bubble formation is determined by values of the *Reynolds* number and the *Weber* number, and also the presence of both the dissolved gas and the cavitation cores in water. In work [12], one obtains a semi-empirical estimation of the cavitation number in the case of incision of the bubble cavitation past the disk depending on the *Reynolds* number $Re = VD_n/\nu$, where D_n is the disk diameter:

$$\sigma = 0.44 + 0.0036 Re^{1/2}, \quad (1)$$

$$Re < 2 \cdot 10^5.$$

According to formula (1), the bubble cavitation past the disk occurs in the range of the cavitation number $\sigma = 0.8 \div 2.0$. With increasing the cavitator motion velocity (or with decreasing the cavitation number), the bubbles merge and eventually form a single attached cavity. It is considered that a developed cavity already exists when $\sigma = 0.5$ [6].

The supercavity formation process can be significantly accelerated by blowing air to the rarefaction zone

past the disk and thereby increasing the cavity pressure, *i.e.* reducing the cavitation number for the same velocity. The supercavity formation processes for a fixed flow velocity and a variable air-supply were studied experimentally in [13–15]. It has been established that the value of the air-supply coefficient $\bar{Q}_{in} = \dot{Q}_{in}/VD_n^2$ required for the cavity formation depends on the *Froude* number $Fr = V/\sqrt{gD_n}$, and this dependence is non-monotonic. So, according to the results of work [13], \bar{Q}_{in} is increased from 0.13 to 0.15 when Fr increases from 5 to 9, and then \bar{Q}_{in} is decreased from 0.15 to 0.07 when Fr increases from 10 to 18. It was also shown that the processes of both the cavity formation and the cavity collapse have a hysteresis form when the air-supply into the cavity increases and decreases.

The processes of development of unsteady ventilated supercavities were numerically modeled using CFD methods [16, 17]. The ventilated cavity reaction to both increasing and decreasing the air-supply is modeled in work [16]. In work [17], the cavitator motion near the free water surface was considered, so that the cavity was ventilated in a natural way by suction of the atmospheric air.

3. Peculiarities of unsteady ventilated supercavities in ponderable fluid

As is known, for small magnitudes of the *Froude* number the gravity influence onto the supercavity consists in bending its axis upwards (so called the cavity floating-up, see Fig. 1). The cavity axis deformation under the gravity influence can be calculated by formula [18]:

$$\bar{h}_g(x) = \frac{(1+\sigma)\bar{x}^2}{3Fr_l^2}, \quad Fr_l = \frac{V}{\sqrt{gL_c}}, \quad (2)$$

where $\bar{h}_g = h_g/L_c$; $\bar{x} = x/L_c$; Fr_l is the *Froude* number with respect to the cavity length.

In this case, the velocity circulation Γ directed counter-clockwise takes place around the cavity in the ponderable fluid [1]:

$$\Gamma = \oint \vec{V} d\vec{s} \approx \frac{g\pi D_c^2}{4V}, \quad (3)$$

where D_c is the cavity mid-section diameter. As a result, the transversal force acts onto the cavity directed downwards and balancing the *Archimedean* lift force. One can show that in the ponderable fluid the maximally admissible pressure in the cavity or the minimal cavitation number exists:

$$\sigma \geq \frac{gD_c}{V^2}, \quad p_c < p_w - \frac{\rho g D_c}{2}. \quad (4)$$

Thus, even for maximal air-supply into the cavity the cavitation number smaller than σ_{min} can not be obtained.

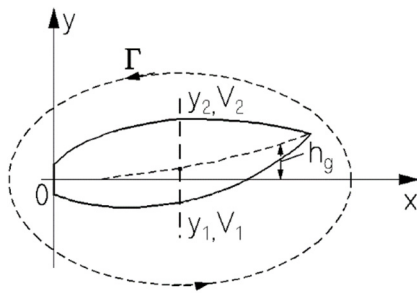


Fig. 1. Scheme of a supercavity in ponderable fluid

The air-loss from a ventilated cavity in the steady flow is defined by the flow behavior in the cavity closure zone. When the cavity closes free, two main types of air-loss may be realized according to the *Campbell–Hilborn* empirical criterion [2]:

$$\sigma Fr \approx 1, \tag{5}$$

where $\sigma = 2(p_w - p_c) / \rho V^2$ is the cavitation number; $Fr = V / \sqrt{g D_n}$ is the Froude number; D_n is the cavitator diameter. Values $\sigma Fr > 1$ corresponds to the first (portion) air-loss type, values $\sigma Fr < 1$ corresponds to the second air-loss type (or air-loss by vortex tubes).

For the first type of air-loss, the approximation formula was proposed [4]:

$$\dot{Q}_{out} = C_f V D_c L_c = C_f V \frac{A D_n^2 c_x}{\sigma \sqrt{\sigma}}, \tag{6}$$

where $\dot{Q}_{out}(t)$ is the volumetric air-loss rate from a cavity; $C_f \approx 0.013$ is the empirical coefficient. For the second type of air-loss, the semi-empirical formula by *L.A. Epshtein* [2] is supposed the most reliable:

$$\bar{Q}_{out} = \frac{0.42 c_{x0}^2}{\sigma (\sigma^3 Fr^4 - 2.5 c_{x0})}, \quad \bar{Q}_{out} = \frac{\dot{Q}_{out}}{V D_n^2}, \tag{7}$$

where c_{x0} is the coefficient of the cavitator drag when $\sigma = 0$ (for the disk-cavitator $c_{x0} = 0.82$).

When calculating unsteady supercavitation flows with the low accelerations, the laws (6), (7) are also applied in the quasi-steady approximation.

However, as experiments have shown, criterion (5) does not work in the case of accelerated motion of the supercavitating models (see below). Namely, in this case the portion air-loss type is preserved when $\sigma Fr < 1$. This can be explained by the fact that in the accelerated motion the flow at the cavity aft zone does not have time to be rearranged under the gravity influence. In this case the air-supply and the air-loss are not balanced: $\dot{Q}_{in} \neq \dot{Q}_{out}$, and it affects on the cavity growth speed.

However, after the flow velocity becomes constant,

the vortex tubes are formed in the cavity aft zone under the gravity influence, by which air is entrained from the cavity. In this case we have $\dot{Q}_{in} = \dot{Q}_{out}$. In the experiments described below, the air-loss from steady supercavities was always realized by the vortex tubes.

The cavity development during the model acceleration may be accelerated by increasing the air-supply rate into the cavity \dot{Q}_{in} . However, in this case the dynamic properties of gas-filled cavities [19, 20] will influence on the cavity behaviour. It was shown that when a certain critical value of the parameter $\beta = \sigma_v / \sigma$ (where σ_v is the vapor cavitation number) is exceeded, the cavity loses its stability and begins to pulsate intensively. The theoretical critical value is $\beta_{cr} = 2.645$, it was obtained for the “slender” supercavities with the large aspect ratio. In this case, the air-loss rate \dot{Q}_{out} is increased appreciably, which prevents further growth of the average cavity length. This circumstance together with relation (4) restricts the ventilated supercavity length achievable for the given parameters.

4. Experimental setup

A series of experiments was carried out for studying the process of formation and development of a separated cavitation flow past a disk cavitator during its acceleration from the state of rest to a steady velocity.

Experimental studies were performed in the high-speed experimental tank at the Institute of Hydromechanics of the National Academy of Sciences of Ukraine. The high-speed experimental tank has length of 140 m, width of 4 m, and depth of 1.8 m. Experimental studies were carried out in accordance with the methods [21] by performing towing tests of cavitator models at the towing velocities up to 10 m/s.

To create a cavity, a disk cavitator with a sharp edge with diameter of $D_n = 30$ mm was used. The cavitator was mounted to the suspension with the help of a threaded adapter, its scheme is shown in Fig. 2.

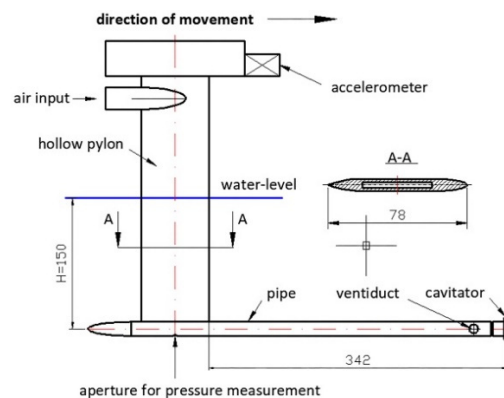


Fig. 2. Scheme of suspension of the cavitator to the towing system of the experimental tank

The suspension consisted of a hollow pylon with 7 mm thick, in the upper part of which there were elements for mounting it to the towing carriage of the experimental tank. The lower part of the pylon was connected to a horizontal pipe with an outer diameter of 16 mm. The internal hollows of the pylon and the pipe had free communication with each other. The ventiducts were made in the frontal part of the pipe behind the threaded adapter to supply air directly to the area past the cavitator.

Air was forcedly supplied to the cavity using a 6-staged axial fan. The air rate measurement was realized using a Honeywell AWM720P1 air rate sensor, which was mounted at the inlet of the axial fan.

In addition, a drainage tube with the diameter of 4 mm was laid through the inner hollow of the pylon. Its lower end was brought out approximately into the middle part of the suspension, and its upper end was connected to the pressure sensor. The cavity pressure was measured using a Motorola MPXV5004DP differential pressure sensor.

The cavitator immersion depth H was regulated by vertical relocation of the whole pylon and was set at the level $H = 150$ mm during these experiments. In this case, the static pressure in water is $p_w = 99.52$ kPa.

At the pylon top, an accelerometer Analog Devices ADXL203 was installed, which was used to record the acceleration value $a = V'$ during speeding-up of the towing carriage of the experimental tank. The current velocity of the carriage V and the distance passed L at the time instant t were calculated by the formulae:

$$V = \int_0^t a(\tau) d\tau, \quad L = \int_0^t V(\tau) d\tau. \quad (8)$$

The towing system of the experimental tank was set up in such a way that the acceleration of the towing carriage from the state of rest to the steady velocity $V = 7.12$ m/s was realized according to an acceleration law close to trapezoidal. Fig. 3 shows graphs of the kinematic characteristics of the towing carriage (the acceleration V' , the velocity V , and the relocation L) during acceleration.

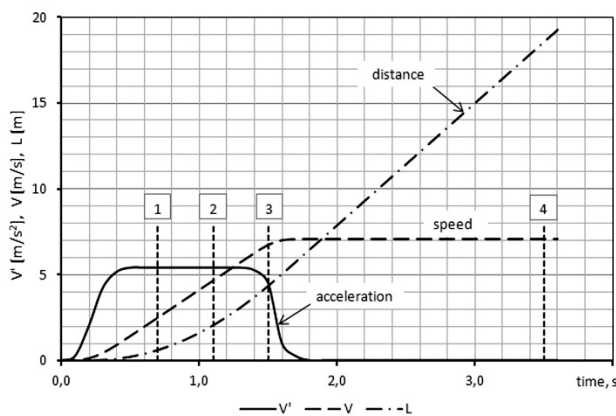


Fig. 3. Kinematic characteristics of the towing carriage when it is accelerated from the state of rest

All sensors and the accelerometer were included in the automated system for collecting and processing information from the experimental tank [22].

To determine the cavity shape past the cavitator, underwater backlight photography was used. To organize back lighting on the measuring part of the experimental tank, a light screen was mounted in the direction of towing carriage motion. The light screen was made of translucent milky plastic and had dimensions of 1000x3000 mm. Approximately 1/3 of the light screen was located above the water surface, and 2/3 of the screen was located under water. The light screen was illuminated by underwater luminaires, which were installed along the tank board and provided uniform illumination of the underwater part of the screen along its whole length. The appearance of the light screen in working condition is shown in Fig. 4.



Fig. 4. Appearance of the light screen in working condition

To determine the cavity shape and its dimensions in the horizontal plane (bottom view), the well-known method of photographing with the help of an underwater mirror installed on the bottom of the experimental tank was used. An underwater mirror 500 mm wide and 3000 mm long was hermetically mounted in a special lever-turn mechanism.

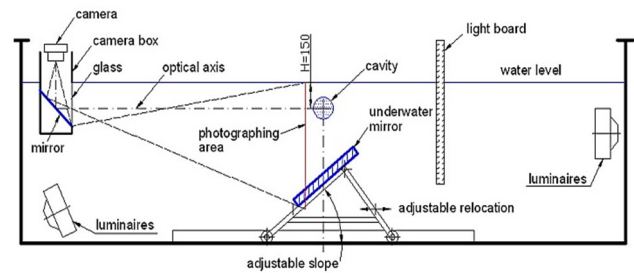


Fig. 5. Scheme of photographing the cavity in the experimental tank

The underwater mirror, together with the lever-turn mechanism was installed on the tank bottom (see Fig. 5). The lever-turn mechanism made it possible to relocate the underwater mirror across the tank and turn it along the longitudinal axis. Using a lever-turn mechanism, the mirror was set in such a way that when photographing the cavity

from the camera box, one half of the frame was occupied by the side view of the cavity, and the other half of the frame was occupied by the bottom view of the cavity, which was reflected in the underwater mirror. This method of photographing allowed the cavity contour parameters to be determined with accuracy ± 1 mm.

5. Experimental results

During all the experiments described below, the axial fan was tuned in such a way that the air-supply rate to the cavity was fixed and was equal to $\dot{Q}_{in} = 2.91$ l/s. Fig. 6 shows the beginning and development of a separated cavitation flow at the initial stage of the towing carriage motion.

At the starting time instants, the separated flow past the cavitator is weakly developed. Therefore, air is not supplied into the zone past the cavitator (see Fig. 6, a). Such a flow pattern is observed on the motion distance equal to about $3 D_n$. Then, the separated flow develops past the cavitator, and zone past the cavitator is saturated with air bubbles (see Fig. 6, b).

The cavity formation is begun when the cavitator passes a distance equal to approximately $10 D_n$. In this case, the cavity formation begins from its upper part (see Fig. 6, c).

A developed supercavitation covering the whole zone

past the cavitator is formed when passing the distance about $15 D_n$ (see Fig.6, d). Below, the process of development of the supercavitation flow is considered in detail on the acceleration distances when the cavity is already formed and covers the whole zone past the cavitator.

Fig. 7 shows the parameters of the supercavitation flow after distance $L = 613$ mm (about $20 D_n$) from the starting point. In Fig. 3, this position is indicated by the number $\boxed{1}$. At this time instant, the cavitator moved with the acceleration $V' = 5.40$ m/s² and the velocity $V = 2.50$ m/s.

Here and below, the photographic images of the cavity were processed using the AutoCAD graphics editor (see Fig. 7, b). The results of measurement of both the side contour and the bottom contour of the cavity allow us to conclude that the cross sections of the developing cavity are close to circular. In this case, the portion type of air-loss from the cavity takes place, the cavity in the aft part is essentially unsteady and pulsates.

Knowing the cavity midsection diameter D_c , one can estimate the instantaneous value of the cavitation number using the well-known formula [1, 2]:

$$D_c = D_n \sqrt{\frac{c_{x0}(1+\sigma)}{\kappa\sigma}}, \tag{9}$$

where $\kappa = 0.9 \div 1.0$ is an empirical constant. In this case we have $D_c = 60$ mm, $\sigma = 0.258$, $p_c = 98.715$ kPa.

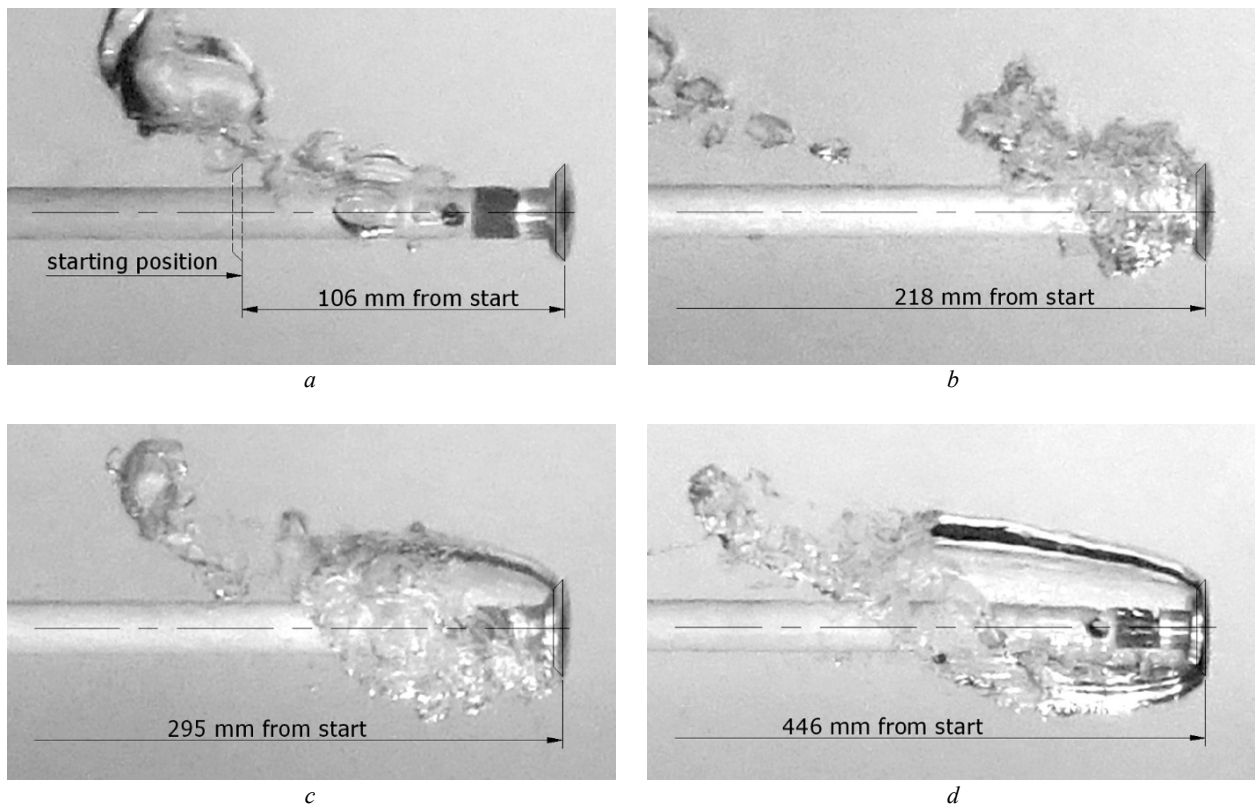


Fig. 6. Formation and development of a separated cavitation flow at the initial stage of the towing carriage motion

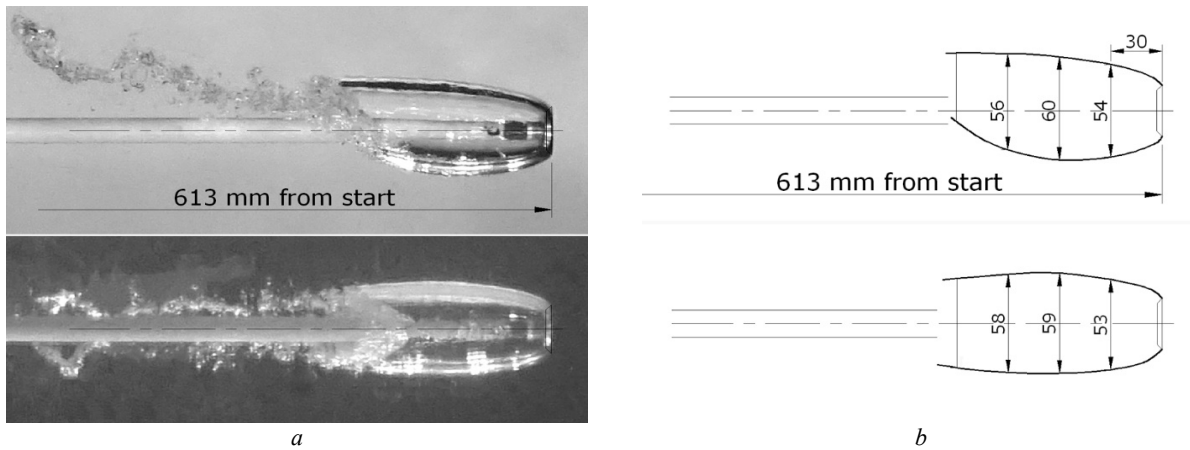


Fig. 7. Supercavitation flow after distance $L = 613$ mm: *a* – cavity view; *b* – cavity sketch

To estimate the effect of the cavitator motion non-stationarity on the supercavitation flow parameters, a series of experiments was carried out with a fixed velocity of the cavitator motion. Fig. 8 shows the parameters of the steady cavitation flow with the same velocity $V = 2.50$ m/s as in Fig. 7. In this case we have $D_c = 64$ mm, and we obtain $\sigma = 0.220$, $p_c = 98.833$ kPa by formula (9). As we can see, the rearrangement of the air-loss type for the same velocity leads to decreasing the cavitation number and, consequently, to increasing the cavity dimensions. This can be explained by increasing the cavity pressure p_c due to decreasing the intensity of the air-loss from the cavity \dot{Q}_{out} , when the air-supply \dot{Q}_{in} is fixed.

As one can see, in this case, air-loss from the cavity is realized by two vortex tubes. In this case, the cavity is stable and its contours are clearly visible. On the cavity frontal part, the cavity cross-sections are close to circular ones (see Fig. 8, *b*). However, past the mid-section, the cavity cross-sections become elliptical and degenerate into

two vortex tubes closer to the cavity aft.

Fig. 9 shows the parameters of the supercavitation flow after distance $L = 2050$ mm from the starting point. In Fig. 3, this position is indicated by the number 2. At this time instant, the cavitator moved with the acceleration $V' = 5.40$ m/s² and the velocity $V = 4.70$ m/s. In this case $D_c = 74$ mm, and we obtain the estimation by formula (9): $\sigma = 0.156$, $p_c = 97.798$ kPa.

One can see that the cavity has significantly increased in both length and diameter in comparison with the previous position. In this case, the shape of the cavity cross-sections remains close to circular along the whole cavity length, and the portion type of air-loss from the cavity is preserved. As a result, the cavity aft part does not have clear outlines.

Fig. 10 shows the parameters of the steady supercavitation flow with the same velocity $V = 4.70$ m/s as in Fig. 9 for comparison. In this case $D_c = 91$ mm, and we obtain by formula (9) the estimation $\sigma = 0.097$, $p_c = 98.449$ kPa.

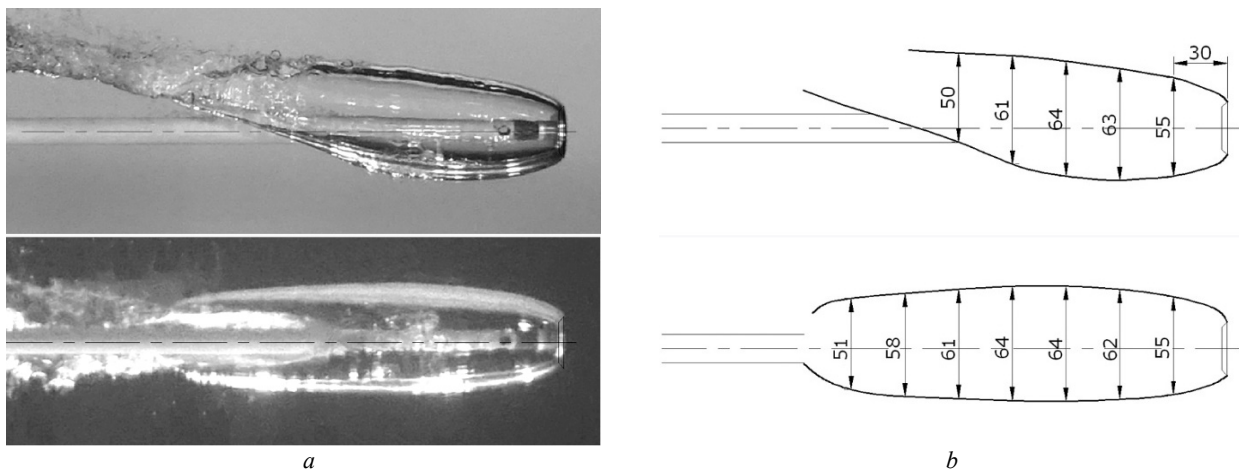


Fig. 8. Steady supercavitation flow with velocity $V = 2.50$ m/s: *a* – cavity view; *b* – cavity sketch

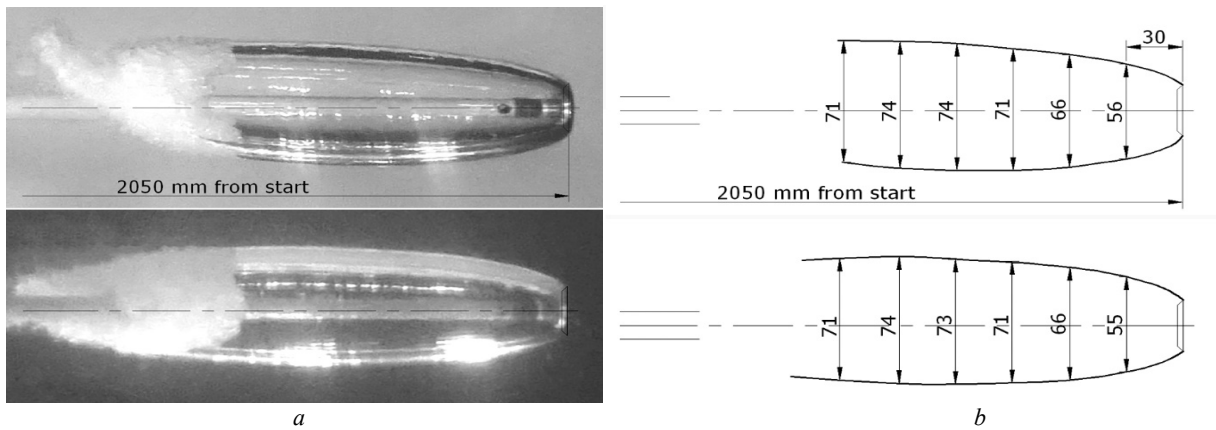


Fig. 9. Supercavitation flow after distance $L = 2050$ mm: *a* – cavity view; *b* – cavity sketch

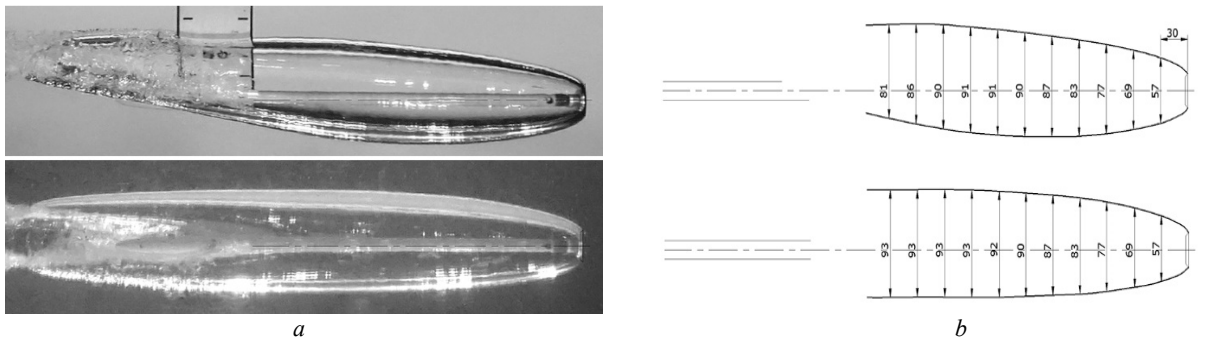


Fig. 10. Steady supercavitation flow with velocity $V = 4.70$ m/s: *a* – cavity view; *b* – cavity sketch

Fig. 11 shows the parameters of the supercavitation flow after distance $L = 4350$ mm from the starting point. In Fig. 3, this position is indicated by the number 3. This time instant corresponds to end of the acceleration process and transition to the steady motion: the cavitator moved with the acceleration $V' = 4.50$ m/s² and the velocity $V = 6.77$ m/s. In this case $D_c = 90$ mm, and we obtain by formula (9) the estimation $\sigma = 0.100$, $p_c = 97.229$ kPa.

It can be seen that the cavity continues to increase in both length and diameter in comparison with the previous

position. In this case, the shape of the cross-sections remains close to circular, and the portion type of air-loss from the cavity is preserved. As a result, the cavity aft part does not have clear outlines.

Fig. 12 shows the parameters of the steady supercavitation flow with the close velocity $V = 7.12$ m/s for comparison. In Fig. 3 this position is indicated by the number 4. In this case $D_c = 112$ mm, and we obtain by formula (9) the estimation $\sigma = 0.063$, $p_c = 97.924$ kPa.

In this experiment, the pressure was measured in the

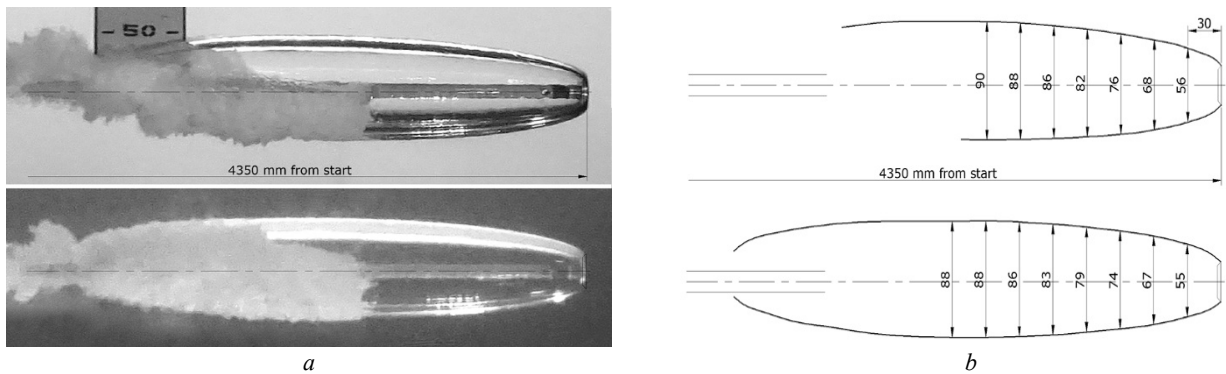


Fig. 11. Supercavitation flow after distance $L = 4350$ mm: *a* – cavity view; *b* – cavity sketch

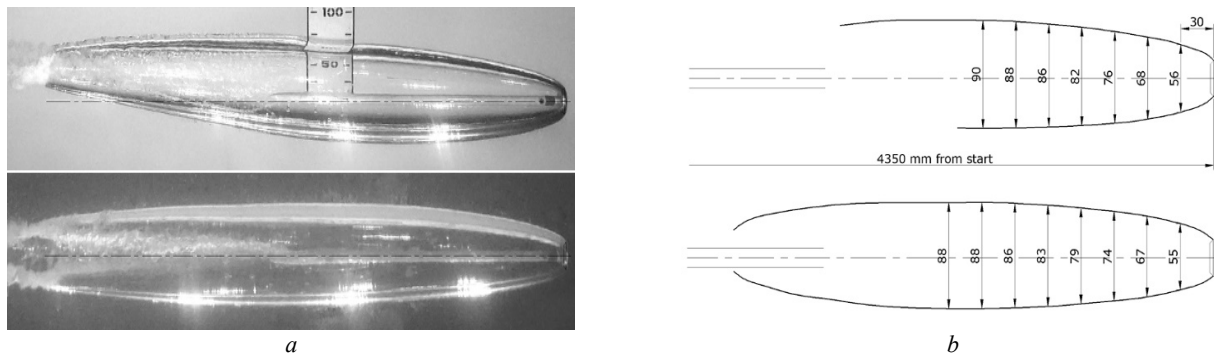


Fig. 12. Steady supercavitation flow with velocity $V = 7.12$ m/s: a – cavity view; b – cavity sketch

middle part of the cavity. In this case, the indication of the differential pressure sensor was $p_c - p_{atm} = -1.036$ kPa, i.e. $p_c = 97.014$ kPa. When immersion depth of the cavitator axis is $H = 150$ mm, and taking into account some increasing the level of the free water surface, the measured cavitation number is $\sigma = 0.071$.

Comparing Fig. 12 with Fig. 11, Fig. 10 with Fig. 9, and Fig. 8 with Fig. 7 shows that in all cases the steady cavity length is almost twice greater than the unsteady cavity length during acceleration for the same velocity. The air-loss from the steady cavities is realized by two vortex tubes, but the portion air-loss is realized from the unsteady cavities. The cross-sections of the unsteady cavity remain circular along the whole length of the cavity. The cross-sections of steady cavities remain circular from the cavitator up to the cavity mid-section, behind the midsection they become elliptical, and closer to the aft the cavities degenerate into two vortex tubes.

Thus, shapes of the cavity aft part differ significantly during acceleration and in the steady motion for the same velocity. In this case, it takes a certain time to rearranging the air-loss type and the cavity formation to dimensions corresponding to the steady motion after termination of acceleration. Significant increasing the cavity length after changing the air-loss type for the fixed air-supply rate \dot{Q}_{in} may be explained by the fact that the air-loss from the steady cavity \dot{Q}_{out} becomes less than the air-loss from the unsteady cavity.

Fig. 13 shows the combined sketches of the side profiles of the frontal part of the unsteady cavity, which were fixed during the cavitator acceleration. The designation of the cavity profiles corresponds to the positions of the cavitator during acceleration in Fig. 3.

Also, the cavity center line is plotted in Fig. 13. It connects the centers of the cavity cross-sections and characterizes intensity of the cavity floating-up under the action of buoyancy. One can see that intensity of the cavity cross-section floating-up is approximately the same at all motion stages. This suggests that the ratio of the hydrodynamic forces and the buoyancy forces is preserved at all stages of the cavity formation.

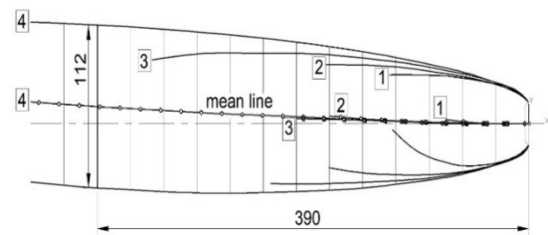


Fig. 13. Combined sketches of the unsteady cavity side profiles

6. Mathematical model

To calculate the unsteady cavity shape in the accelerated model motion, we used the approximation mathematical model based on the *G.V. Logvinovich* principle of independence of the cavity section expansion [1]. The expression for the cross-section area of an unsteady axisymmetric cavity on the its main part has the form [3]:

$$S(\tau, t) = S_1 + \frac{k_1}{4} AD_n V(\tau) \sqrt{c_{x0}} (t - \tau) - \frac{k_1}{2} \int_{\tau}^t (t - s) \sigma(\tau, s) ds, \quad x > x_1, \quad (10)$$

where $S_1(x_1)$ is area of the “matching section” of the cavity frontal part and the cavity main part; $k_1 = 4\pi / A^2$; $A \approx 2.0$ is the empiric constant. The shape of the cavity frontal part is calculated by empiric formula [1]:

$$S(x) = \pi R_n^2 \left(1 + \frac{3x}{R_n} \right)^{\frac{2}{3}}, \quad 0 < x \leq x_1 \quad (11)$$

The best agreement with experimental data is attained when $x_1 = D_n$. The cavity axis distortion under the gravity influence is calculated by formula (2).

The unsteady cavity pressure $p_c(t)$ at each time instant can be calculated from equation of the gas mass balance in the cavity [19]:

$$\frac{d}{dt} [p_c(t) Q_c(t)] = p_w [\dot{Q}_{in} - \dot{Q}_{out}(t)], \quad (12)$$

where $Q_c(t)$ is the cavity volume; p_w is the static water pressure. The air-loss value is calculated by formulae (6), (7).

As the experience of using this mathematical model shows, it gives good results for sufficiently low values σ and relatively high values of the velocity V . Our works [23, 24] are devoted specially to the experimental verification of this mathematical model.

However, in this case of accelerated motion and relatively low velocities $V \leq 7.12$ m/s, which are typical for the experiments described above, attempt of its application gave unsatisfactory results. The reason is that values of the parameter β much exceed its critical value for low values of V and high values of p_c , the cavities rapidly lose stability and begin to pulsate intensely. In this case, the growth of the mean cavity length is ceased. However, such pulsations of ventilated cavities were not observed in our experiments.

In order to match the calculation results with the experiment, the following changes were made in the mathematical model (10)–(12):

1) It is accepted that the portion type of air-loss from the cavity (6) is preserved at the stage of the model accelerated motion. After termination of acceleration and reaching the steady motion with the fixed velocity V_1 , the type of air-loss changes to the gas loss by vortex tubes (7) after a certain time T .

2) For the purpose of prevention of the cavity self-induced oscillation, a specified law of the cavity pressure monotonic variation (particularly, the condition $p_c = const$) is accepted instead of equation (12).

The validity of these assumptions could be verified by comparing the computer simulation results with the experimental data.

7. Computer simulation

The described calculation method is implemented in the SCV computer program, which makes it possible to display the calculation results on the screen “in real time”. As in the experiment, the model is a disk cavitator with dia-

meter $D_n = 30$ mm. Fig. 14 shows the calculated shape of a steady ventilated cavity after termination of acceleration ($H = 0.15$ m; $V = 7.12$ m/s; $\sigma = 0.071$, see Fig. 12).

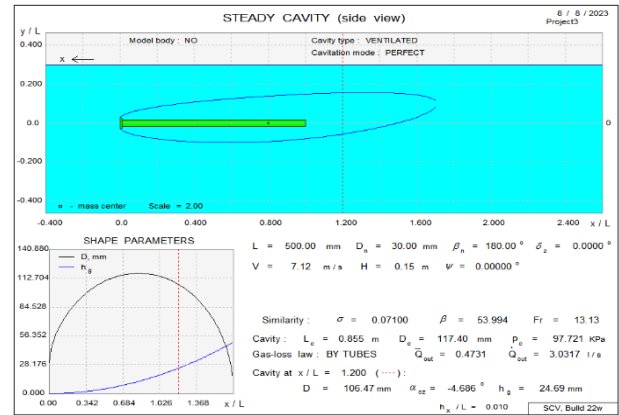


Fig. 14. Shape and parameters of the steady cavity after termination of acceleration

Table 1 and Table 2 compare the experimental shape and the calculated shape of the steady ventilated cavity after termination of acceleration.

In the calculation, the air-loss from the steady cavity is realized by the vortex tubes according to criterion (5), as in the experiment (see Fig. 12). It is assumed in this mathematical model that the cavity sections remain circular ones along the whole cavity length. Therefore, as expected, we have a sufficiently close correspondence to the experiment for the cavity shape up to the cavity midsection and growing discrepancies behind the midsection. According to formula (7), we obtain the air rate $\dot{Q}_{out} = \dot{Q}_{in} = 3.03$ l/s, which is close to the air-supply rate in the experiment 2.91 l/s.

To verify the accepted mathematical model, calculations with the parameter values corresponding to the experiments were performed. The parameters corresponding to Fig. 7, when equation (10) can already be applied, were accepted as the starting parameters (see Fig. 3, position [1]): $V_0 = 2.5$ m/s; $D_0 = 60$ mm; $\sigma = 0.258$. In calculation, the air-supply into the cavity was considered to be fixed:

Table 1. The steady cavity shape, experiment Fig. 12

x , mm	60	120	180	240	300	360	420	480
D , mm	70	87	99	106	111	112	111	107
h_g , mm	0	2	4	6	8	10	13	17

Table 2. The steady cavity shape, calculation Fig. 14

x , mm	60.0	120.0	180.0	240.0	300.0	360.0	420.0	480.0
D , mm	69.76	87.35	99.41	107.82	113.38	116.50	117.39	116.09
h_g , mm	0.26	1.03	2.32	4.12	6.44	9.27	12.61	16.48

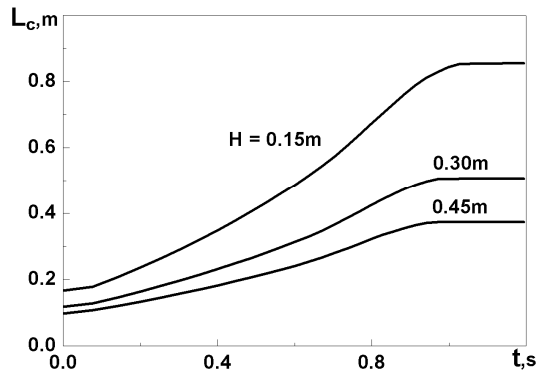


Fig. 19. Influence of the cavitator immersion depth on the cavity growth during acceleration

One can see that increasing the immersion depth leads to decreasing the growing cavity dimensions owing to increasing the static water pressure p_w . But it practically does not influence on the cavity growth speed.

8. Conclusion

Summarizing the results of the performed experimental studies, one can state that the cross sections of the unsteady cavity are close to circular ones along the whole cavity length and at all stages of acceleration. During the cavitator acceleration from a state of rest, the portion air-loss from the cavity is preserved, although the air-loss by vortex tubes is realized in the steady motion regimes with

the same velocities. This leads to that the shapes of the cavity aft part are significantly different during acceleration and in the similar steady motion. A certain time is required to rearranging the air-loss type and the cavity formation to dimension corresponding to the steady motion after termination of acceleration. After rearranging, the cavity length increases almost twice at the same both the velocity and the air-supply rate into the cavity. This indicates essential decreasing the air-loss rate from the cavity.

To describe the second stage of process of the ventilated cavity development during acceleration, the modified mathematical model based on the *G.V. Logvinovich* principle of independence of the cavity section expansion has been proposed. Its features are both the assumption about the preservation of the portion type of the air-loss from the cavity and the assumption that the cavity pressure is fixed during acceleration. To verify the adequacy of the accepted mathematical model, the computer simulation of the ventilated cavity development process during acceleration was performed, which corresponded to the experiments carried out.

Comparison of results of the cavity growth speed calculation by the proposed method with the experimental data has been shown their satisfactory correspondence. This allows this mathematical model to be recommended for computer simulation of the ventilated cavity development process during acceleration in a wide range of parameters. As examples, an analysis of the influence of both the immersion depth and the air-supply rate on the process of the ventilated supercavity development has been performed.

References

- [1] G.V. Logvinovich, *Hydrodynamics of free-boundary flows*, Kyiv, Ukraine: Naukova Dumka, 1969, 208p.
- [2] L.A. Epshtein. *Methods of theory of dimensionalities and similarity in problems of ship hydromechanics*, Leningrad: Sudostroenie Publ., 1970, 207p.
- [3] V.N. Semenenko, *Artificial cavitation. Physics and calculations*, RTO-AVT/VKI Special Course on Supercavitating Flows, February 12–16, 2001, VKI, Brussels (Belgium).
- [4] J.H. Spurk, “On the gas loss from ventilated supercavities”, *Acta Mechanica*, no. 155, pp. 125–135, 2002.
- [5] R.T. Knapp, J.W. Daily, and F.G. Hammitt, *Cavitation*, McGraw-Hill Book Company, NY and al, 1970.
- [6] I.T. Egorov, Yu.M. Sadovnikov, I.I. Isaev, and M.A. Basin, *Artificial cavitation*, Leningrad: Sudostroenie Publ., 1971, 284p.
- [7] G.V. Logvinovich and V.V. Serebryakov, “On methods for calculating a shape of slender axisymmetric cavities”, *J. of Hydro-mechanics*, no. 32, pp. 47–54, 1975.
- [8] V.N. Semenenko and Ye.I. Naumova, “Study of the supercavitating body dynamics”, in *Supercavitation: Advances and Perspectives*. Springer-Verlag, Berlin and Heidelberg, pp. 147–176, 2012. doi: 10/1007/978-3-64223656-3_9
- [9] Yu.N. Savchenko and V.N. Semenenko, “Motion of supercavitating vehicle during underwater speeding-up”, *J. of Applied Hydromechanics*, vol. 17(89), no. 4, pp. 36–42, 2015.
- [10] V.N. Semenenko and O.I. Naumova, “Dynamics of a partially cavitating underwater vehicle”, *Hydrodynamics and Acoustics*, vol. 1 (91), no. 1, pp. 70–84, 2018. doi: 10.15407/jha2018.01.070
- [11] W. Zou, T. Liu, Y. Shi, and J. Wang, “Analysis of motion characteristics of a controllable ventilated supercavitating vehicle under accelerations”, *Journal of Fluids Engineering*, vol. 143, pp. 111204-1–111204-14, November 2021.
- [12] R. E.A. Arndt, “Semiempirical analysis of cavitation in the wake of a sharp-edged disk”, *Journal of Fluids Engineering*, pp. 560–562, September 1976.
- [13] A. Karn, R.E.A. Arndt, and J. Hong, “Gas entrainment behaviors in the formation and collapse of a ventilated supercavity”, *Experimental Thermal and Fluid Science*, vol. 79, pp. 294–300, 2016.

- [14] B.-K. Ahn, S.-W. Jeong, J.-H. Kim, S. Shao, J. Hong, and R.E.A. Arndt, “An experimental investigation of artificial supercavitation generated by air injection behind disk-shaped cavitators”, *Int. J. of Naval Architecture and Ocean Engineering*, 9, pp. 227–237, 2017.
- [15] S. Shao, A. Balakrishna, K. Yoon, J. Li, Y. Liu, and J. Hong, “Effect of mounting strut and cavitator shape on the ventilation demand for ventilated supercavitation”, *Experimental Thermal and Fluid Science*, vol. 118, 2020.
- [16] G. Guohua, Z. Jing, M. Fe, and L. Weidong, “Numerical study on ventilated supercavitation reaction to gas supply rate”, *Advanced Materials Research*, vols. 418–420, pp. 1781–1785, 2012.
- [17] Y. Wang, X. Wu, and C. Huang, “Ventilated partial cavitating flow around a blunt body near the free surface”, in *Proc. Int. Symp. on Transport Phenomena and Dynamics of Rotating Machinery*. Honolulu, Hawaii, 2016.
- [18] V.N. Buyvol, *Slender cavities in flows with perturbations*, Kyiv, Ukraine: Naukova Dumka, 1980, 296 p.
- [19] E.V. Paryshev, “Numerical modeling of pulsation of ventilated cavities”, *Trudy TSAGI*, No. 2272, pp.19–28, 1985.
- [20] V.N. Semenenko, “Computer Modelling of Pulsations of Ventilating Supercavities”, *Int. J. of Fluid Mechanics Research*, 23, (3 & 4), pp. 302–312, 1996.
- [21] “Testing and Extrapolation Methods. High Speed Marine Vehicles. Resistance Test”, *ITTC – Recommended Procedures and Guidelines No. 7.5-02 -05-01*, 25th ITTC, 2008.
- [22] V. Kochin and V. Moroz, “Automated data acquisition and processing system for a high-speed towing tank”, *Modern technologies of automation*, no. 3, pp. 48–50, 2009.
- [23] V. Kochin, V. Moroz, V. Semenenko, and Paik Bu-Geun, “Experimental verification of mathematical model of the supercavitating underwater vehicle dynamics”, in *Proc. The 11th International Symposium on Cavitation CAV2021*, DCC, Daejeon, Korea, May 9–13, 2021.
- [24] V. Semenenko, V. Moroz, V. Kochin, and O. Naumova, “Dynamics of supercavitating vehicles with cone cavitators”, *Mechanics and Advanced Technologies*, vol. 6, no. 1. pp. 85–96, 2022. doi: 10.20535/2521-1943.2022.6.1.252889

Формування та розвиток вентиляваної суперкаверни за дисковим кавітатором при прискореному русі

В. Мороз¹, В. Кочин¹, В. Семененко¹, О. Наумова¹

¹ Інститут гідромеханіки НАН України, Київ, Україна

Анотація. Робота присвячена експериментальному дослідженню та комп'ютерному моделюванню процесу формування та розвитку вентиляваної суперкаверни при прискореному русі дискового кавітатора зі стану спокою до усталеної швидкості. Проведено серію експериментів у швидкісному дослідному басейні Інституту гідромеханіки НАН України за різних значень витрати повітря на піддув каверни. Встановлено, що при горизонтальному прискореному русі завжди зберігається порційний тип виносу газу з каверни, в той час як при усталеному русі з тими ж швидкостями в даних експериментах завжди реалізувався тип виносу газу по вихрових трубках. При цьому форма поперечних перерізів нестационарної каверни близька до кругової по всій довжині каверни та на всіх етапах розгону. Для опису цього процесу запропоновано модифіковану математичну модель, засновану на принципі незалежності розширення перерізів каверни Г.В. Логвіновича. Шляхом комп'ютерного моделювання проведено аналіз впливу глибини занурення та витрати повітря на піддув на процес розвитку вентиляваної суперкаверни при розгоні.

Ключові слова: дисковий кавітатор, вентилявана каверна, прискорений рух, експериментальні дослідження, комп'ютерне моделювання.